INTERNATIONAL JOURNAL FOR NUMERICAL METHODS IN FLUIDS, VOL. 9, 499 515 (1989)

FLAME COMPUTATIONS BY A CHEBYSHEV MULTIDOMAIN METHOD

U. EHRENSTEIN, H. GUILLARD AND R. PEYRET*

*INRIA, Avenue E. Hugues, Sophia-Antipolis, F-06560 Valbonne, France *and Université de Nice, Parc Valrose, F-06000 Nice, France*

SUMMARY

A Chebyshev collocation method is proposed for the computation of laminar flame propagation in a two-dimensional gaseous medium. The method is based on a domain decomposition technique associated with co-ordinate transforms to map the infinite physical subdomains into finite computational ones. The influence matrix method is used to handle the patching conditions at the interfaces. This technique is particularly efficient since at each time step only matrix products have to be performed. The method is tested first on an elliptic model problem; it is then applied to laminar flame computations, including calculations of cellular instabilities of flame fronts.

KEY WORDS Chebyshev collocation Laminar flames Domain decomposition Influence matrix

1. INTRODUCTION

For simple (Cartesian) geometries the efficiency of spectral methods is supported by strong theoretical and numerical evidence (see e.g. References 1–3). An important advantage of these methods is that for smooth solutions of differential problems a high accuracy can be obtained thanks to the rapid (in some cases exponential[4]) rate of convergence of the polynomial approximation. This, combined with the existence of fast transform algorithms, makes spectral methods particularly attractive for a large class of problems. However, spectral methods still suffer from two major drawbacks:

(1) They are restricted to simple geometries.
(2) They are not well suited for problems whose solutions exhibit sharp inner gradients.

One possible remedy resorts to mapping techniques. For problems with complex geometries the use of mapping techniques to reduce the complex physical domain to a simple Cartesian computational domain was first advocated by Orszag.[5] However, this is not always possible to perform in a single map and more elaborate techniques have to be found. The use of mapping procedures can also be useful for problems exhibiting solutions with sharp gradients. This was investigated by Badesvant *et al.*[6] and Brachet[7] using a fixed co-ordinate transform, while Guillard and Peyret[8] and Bayliss and Matkowsky[9] have proposed a self-adaptive procedure to define a mapping adapted to the computed solution. However, in some cases this can lead to expensive computational procedures.

An alternative solution is the use of domain decomposition methods. While for problems with complex geometries they can be simpler to implement than mapping techniques, they can also be

0271-2091/89/050499-17$08.50

Received 11 January 1988
Revised 30 June 1988

very useful for the computation of high-gradient solutions as an adequate resolution of the regions with large variations can be reached by the introduction of additional domains in these regions. According to the classification by Quarteroni,[10] domain decomposition methods may be split into two subgroups: methods of variational type and patching methods.

Methods of the first group use the same variational formulation as the conventional (h-version) finite element method. These methods include the p-version of the finite element method studied by Babuska *et al.*[11] as well as the spectral element method of Patera[12] and the global element method introduced by Delves and Hall.[13]

Instead of the conventional Galerkin formulation, patching methods are based on a collocation procedure. The principle of these methods is simply to collocate the equations at every internal collocation point while continuity of the solution and of the first derivative is enforced on the interface collocation points. From an algorithmic point of view, the linear system arising from the collocation equations can be solved by either an iterative or a direct method. An iterative method for the Helmholtz problem is described in Zanolli[14] and Funaro *et al.*,[15] while a non-iterative method based on the use of the influence matrix technique is proposed in Macaraeg and Streett,[16] Marion[17] and Pulicani.[18] However, in this latter work the solution in each subdomain is obtained by a tau method instead of a collocation one.

The purpose of this paper is to investigate the application of a domain decomposition technique to problems exhibiting sharp gradients, namely flame propagation problems. The proposed method is a direct patching method for the solution of parabolic equations in an infinite domain. It is characterized by the following features:

(1) The domain is split into three subdomains and a co-ordinate transform is performed in the two extreme subdomains in order to map $[-1, 1]$ into a semi-infinite domain.
(2) The inner domain can move to follow a structure of interest.
(3) A Chebyshev collocation procedure is used in each of the three subdomains and the continuity conditions at the interface are imposed via an influence matrix technique.
(4) At each time step the discrete systems are solved by a diagonalization algorithm.

The multidomain method is described in Section 2 while Section 3 is devoted to the presentation and discussion of the numerical results. The efficiency of this numerical procedure is first shown on a model problem. It is then applied to computations of the propagation of one-dimensional flames. Finally the numerical algorithm is used for the computation of cellular instabilities of a two-dimensional flame front propagating into an infinite channel.

2. NUMERICAL METHOD

For the description of the method we shall use the parabolic problem

$$\frac{\partial\theta}{\partial t}-\Delta\theta=\omega(\theta) \quad \text{in} \quad D=]-\infty, +\infty[\times]-a, +a[\tag{1}$$

with the boundary and initial conditions

$$\begin{aligned} &\theta\to 0 && \text{for} \quad x\to-\infty,\\ &\theta\to 1 && \text{for} \quad x\to+\infty,\\ &(\partial\theta/\partial y)=0 && \text{at} \quad y=\pm a,\\ &\theta(x, y, 0)= && \theta^0(x, y). \end{aligned} \tag{2}$$

The domain D is then split into three subdomains defined by (see Figure 1)

$$D_- =]-\infty, x_1[\times]-a, +a[,$$
$$D_0 =]x_1, x_2[\times]-a, +a[,$$
$$D_+ =]x_2, +\infty[\times]-a, +a[.$$

The points x_1 and x_2 delimiting the inner domain are allowed to move with a velocity $U(t) = x_1'(t) = x_2'(t)$. This will permit us to follow a structure of interest (a flame front in Section 3.2) as it moves inside the domain D.

In order to use a Chebyshev collocation method each subdomain is mapped into the square $]-1, +1[\times]-1, +1[$ by a suitable co-ordinate transform:

$$x = g_j(\xi), \qquad y = a\eta, \qquad j \in \{-, 0, +\}. \tag{3}$$

Here the functions g_j are defined by

$$g_-(\xi) = -\delta_- \frac{1-\xi}{1+\xi} + x_1, \qquad g_0(\xi) = \delta_0 \frac{1+\xi}{2} + x_1, \qquad g_+(\xi) = \delta_+ \frac{1+\xi}{1-\xi} + x_2, \tag{4}$$

where δ_j are positive constants; δ_- and δ_+ characterize the slope of the co-ordinate transform at the interfaces x_1 and x_2 respectively, while $\delta_0 = x_2 - x_1$ is the (constant) width of the inner domain. Then in each subdomain the solution θ_j verifies an equation of the type

$$\frac{\partial \theta_j}{\partial t} - A_j U \frac{\partial \theta_j}{\partial \xi} - \Delta_j \theta_j = \omega(\theta_j) \tag{5}$$

with

$$\Delta_j = C_j \frac{\partial^2}{\partial \xi^2} + B_j \frac{\partial}{\partial \xi} + \frac{1}{a^2} \frac{\partial^2}{\partial \eta^2}, \tag{6}$$

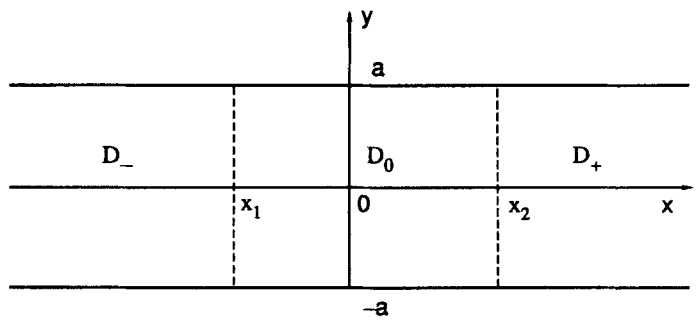

Figure 1. Domain decomposition

where A_j, B_j and C_j are functions of ξ via the mapping $x=g_j(\xi)$. For each transformed subdomain, boundary conditions have to be imposed. The physical boundary conditions (2) become

$$\begin{aligned} &\theta_-(-1,\eta,t)=0,\\ &\theta_+(+1,\eta,t)=1,\\ &(\partial\theta_j/\partial\eta)(\xi,\pm1,t)=0, \quad j\in\{-,0,+\}, \end{aligned} \tag{7}$$

while we have to consider patching conditions at the interfaces $x=x_1$ and $x=x_2$. This can be done in various ways (see Reference 10 for a review). Here we choose (as in References 5 and 18) to enforce the continuity of the function and of its normal derivative at the interface, i.e.

$$\theta_-(1,\eta,t)=\theta_0(-1,\eta,t), \tag{8}$$

$$\frac{2}{\delta_-}\frac{\partial\theta_-}{\partial\xi}(1,\eta,t)=\frac{2}{\delta_0}\frac{\partial\theta_0}{\partial\xi}(-1,\eta,t) \tag{9}$$

for the interface $x=x_1$ and

$$\theta_0(1,\eta,t)=\theta_+(-1,\eta,t), \tag{10}$$

$$\frac{2}{\delta_0}\frac{\partial\theta_0}{\partial\xi}(1,\eta,t)=\frac{2}{\delta_+}\frac{\partial\theta_+}{\partial\xi}(-1,\eta,t) \tag{11}$$

for the interface $x=x_2$.

Equations (5) with the boundary conditions (7), the patching conditions (8)–(11) and the initial condition

$$\theta_j(\xi,\eta,0)=\theta_j^0(\xi,\eta) \tag{12}$$

completely determine the problem.

Equation (5) is then advanced in time by a second-order Adams–Bashforth/backward Euler scheme:

$$\frac{3\theta_j^{n+1}-4\theta_j^n+\theta_j^{n-1}}{2\delta t}-A_j\left[2U^n\left(\frac{\partial\theta_j}{\partial\xi}\right)^n-U^{n-1}\left(\frac{\partial\theta_j}{\partial\xi}\right)^{n-1}\right]-\Delta_j\theta_j^{n+1}-(2\omega_j^n-\omega_j^{n-1})=0. \tag{13}$$

At each time step this reduces the problem to a linear elliptic equation of the type

$$\Delta_j\theta_j-\sigma\theta_j=E_j \tag{14}$$

with the boundary conditions (7) and the interface conditions (8)–(11).

The main difficulty of the above problem is to enforce the interface conditions in an efficient way. Iterative procedures can be used as done in References 14 and 15; however, for unsteady problems the use of a direct method leaving the major part of the computations in a preprocessing stage could be of interest. Hence for this problem we have used the so-called influence matrix technique. This technique has become popular in spectral methods since the work of Kleiser and Schumann[19] who applied it for handling the incompressibility conditions and related boundary conditions for pressure using the Navier–Stokes equations. This method has often been used in various circumstances, in particular for Chebyshev domain decomposition.[16] However, to our knowledge, the method has only been described for one-dimensional problems[10,18]. Here,

although the problem is two-dimensional, the domain decomposition is made in one direction, so that the basic principles remain of a one-dimensional nature. Therefore in the following we briefly describe the technique, emphasizing only the particulars associated with the two-dimensionality of the global problem.

First we write the solutions θ_j as the sum of two functions:

$$\theta_j = \tilde{\theta}_j + \bar{\theta}_j.$$

$\tilde{\theta}_j$ are the solutions of equation (14) with the boundary conditions

$$\begin{aligned} &\tilde{\theta}_-(-1,\eta)=0, \quad &&\tilde{\theta}_-(+1,\eta)=0,\\ &\tilde{\theta}_0(-1,\eta)=0, \quad &&\tilde{\theta}_0(+1,\eta)=0,\\ &\tilde{\theta}_+(-1,\eta)=0, \quad &&\tilde{\theta}_+(+1,\eta)=1,\\ &\frac{\partial\tilde{\theta}_j}{\partial\eta}(\xi,\pm1,t)=0, \quad &&j\in\{-,0,+\} \end{aligned} \tag{15}$$

and then they satisfy the physical boundary conditions (7) and the interface conditions (8) and (10). However, they do not satisfy the interface conditions (9) and (11). The enforcement of these conditions is obtained via the correction terms $\bar{\theta}_j$ which are solutions of the homogeneous elliptic equation

$$\Delta_j\bar{\theta}_j - \sigma\bar{\theta}_j = 0 \tag{16}$$

with the boundary conditions

$$\begin{aligned} &\bar{\theta}_-(-1,\eta)=0,\\ &\bar{\theta}_-(+1,\eta)=h_-(\eta),\\ &\bar{\theta}_0(-1,\eta)=h_-(\eta),\\ &\bar{\theta}_0(+1,\eta)=h_+(\eta),\\ &\bar{\theta}_+(-1,\eta)=h_+(\eta),\\ &\bar{\theta}_+(+1,\eta)=0,\\ &\frac{\partial\bar{\theta}_j}{\partial\eta}(\xi,\pm1)=0, \quad j\in\{-,0,+\}. \end{aligned} \tag{17}$$

We note that for any functions h_- and h_+, $\theta_j=\tilde{\theta}_j+\bar{\theta}_j$ are solutions of equation (14) with the physical boundary conditions (7) and they satisfy the continuity conditions at the interfaces (8) and (10). However, the continuity conditions (9) and (11) of the derivatives at the interfaces are not automatically satisfied for any h_- and h_+. Thus we now have to define these functions in such a way that these conditions are verified.

For this we need to enter into the description of the spatial approximation. Let $P_{N,M}$ be the set of polynomials of degree at most N in ξ and M in η. The solution θ_j is assumed to belong to $P_{N_j,M}$, where N_j is the degree of the approximation in ξ in the subdomain D_j. This solution is calculated by a collocation method based on the Chebyshev points:

$$\begin{aligned} &\xi_n=\cos\frac{n\pi}{N_j}; \quad n=0,\ldots,N_j, \quad j\in\{-,0,+\},\\ &\eta_m=\cos\frac{m\pi}{M}; \quad m=0,\ldots,M. \end{aligned} \tag{18}$$

For any function $\phi_j(\xi, \eta)$ its derivatives at the collocation points can be expressed as the derivatives of the polynomial that interpolates ϕ_j on the collocation points. The collocation method (see e.g. Reference 20) consists of satisfying the differential equations at the inner collocation points. This gives a set of algebraic equations for the values $\phi_j(\xi_n, \eta_m)$ at the collocation points which is closed by adding the boundary conditions.

This collocation method is first applied to solve the mixed Dirichlet–Neumann problem defined by (14), (15) for each $\tilde{\theta}_j$. The resulting algebraic system is solved by a full matrix diagonalization algorithm[21,22] similar to the one considered in Reference 23 for the tau–Chebyshev method. In this method the major part of the computation is done in a preprocessing stage before the start of the time integration. Then at each time step the computation is reduced to simple matrix products.

We now need to solve the problem (16), (17) for the θ_j and to define the functions h_- and h_+, which are given in the collocation approximation by their nodal values $h_-(\eta_m)$ and $h_+(\eta_m)$, $m=1, \ldots, M-1$, in such a way that the continuity conditions (9) and (11) are satisfied.

To do that, we write the functions $\bar{\theta}_j$ as the sum of elementary solutions $u_{\pm}^m$ and $u_{0,\pm}^m$ belonging to $P_{N_j,M}$, $1 \leqslant m \leqslant M-1$:

$$\bar{\theta}_j = \sum_{m=1}^{M-1} h_j(\eta_m) u_j^m \quad \text{for} \quad j \in \{-, +\}, \tag{19}$$

$$\bar{\theta}_0 = \sum_{j \in \{-,+\}} \sum_{m=1}^{M-1} h_j(\eta_m) u_{0,j}^m. \tag{20}$$

The time-independent polynomial functions $u_j^m, u_{0,j}^m, j \in \{-, +\}$, are solutions of the homogeneous equation (16) with homogeneous Neumann conditions at the boundaries $\eta = \pm 1$ and homogeneous Dirichlet conditions at the boundaries $\xi = \pm 1$, except at the interfaces between the subdomains where

$$u_{\pm}^m(\mp 1, \eta_k) = \delta_{k,m} \quad (k, m = 1, \ldots, M-1), \tag{21}$$

$$u_{0,\pm}^m(\mp 1, \eta_k) = \delta_{k,m} \quad (k, m = 1, \ldots, M-1), \tag{22}$$

with $\delta_{k,m}$ the Kronecker symbol. The problems defining these elementary solutions are solved by the collocation method associated with a full diagonalization procedure as done for the calculation of $\tilde{\theta}_j$.

Writing down the continuity conditions (9) and (11) for the ξ-derivatives at each collocation point located on the interface gives a linear system

$$\mathbf{AH} = \mathbf{G}, \tag{23}$$

where $\mathbf{H}$ is the vector of the unknowns $h_{\pm}(\eta_m)$, $m=1, \ldots, M-1$. $\mathbf{G}$ depends only on the ξ-derivatives of $\tilde{\theta}_j$. The influence matrix $\mathbf{A}$ depends only on the ξ-derivatives of the elementary solutions and hence can be computed and inverted once and for all at the beginning of the computation. Solving (23) gives the $h_j(\eta_m)$ and then the required correction term $\bar{\theta}_j$.

The global algorithm is thus composed of the following steps:

(1) In a preprocessing stage the solutions $u_{\pm}^m, u_{0,\pm}^m$ are computed and stored, then the matrix $\mathbf{A}$ is computed and inverted.
(2) At each time step the system (14), (15) is solved for each $\tilde{\theta}_j$.
(3) With these solutions the right-hand side of the linear system (23) is computed and the vector $\mathbf{H}$ is obtained by multiplication by the inverse of the influence matrix.
(4) Equations (19) and (20) give the correction terms $\bar{\theta}_j$.
(5) Finally the solution is obtained by adding the two components $\tilde{\theta}_j$ and $\bar{\theta}_j$.

3. NUMERICAL RESULTS

3.1. An elliptic model problem

We consider the problem

$$\Delta u - \sigma u = f \tag{24}$$

with homogeneous Dirichlet boundary conditions in x and homogeneous Neumann boundary conditions in y. The function f is chosen such that the exact solution of (24) is $u = e^{-x^2}\cos(\pi y)$ with $\sigma = 10$.

The spectral multidomain method described above is then applied to (24) with the following domain decompositions:

$$\text{decomposition 1: } D_0 =]-1, +1[\times]-1, +1[,$$
$$\text{decomposition 2: } D_0 =]-2, +2[\times]-1, +1[.$$

For both cases the values $\delta_- = \delta_+ = 1$ have been considered in the co-ordinate transforms and the number of polynomials in the y-direction is equal to 17. Table I shows the evolution of the error as the number of polynomials is increased in each of the subdomains.

Table I. Evolution of the error for the model problem. E_1^∞ and E_2^∞ are the discrete maximum errors on the collocation points for decompositions 1 and 2 respectively

N_-	N_0	N_+	E_1^∞	E_2^∞
6	10	6	2·73(−3)	1·11(−3)
12	20	12	2·26(−4)	2·42(−6)
20	30	20	5·25(−6)	3·80(−8)
20	40	20	5·25(−6)	3·80(−8)
30	40	30	1·52(−7)	4·65(−10)

It can be observed that decomposition 2 gives better results than decomposition 1. This means that the extent of the inner domain plays an important role in the overall accuracy: the location of the interface with respect to the large-gradient zone is critical. Table I shows that a good accuracy is obtained even with a very small number of polynomials. By comparing the last three rows, it appears that a highly accurate representation of the solution requires a sufficiently large numbers of polynomials in the outer domains even if the solution is quite smooth in those regions and decays very rapidly. It is possible that the stretching to infinity (4) is responsible for this situation and a domain truncation could possibly give better results. In fact it has been shown[24] that domain truncation gives better convergence than mapping to approximate the function e^{-x^2} when the length L of the finite domain and the analogue of the parameters $\delta_\pm$ in (4) are optimally chosen. On the other hand, as experienced by Grosh and Orszag[25] and justified by Boyd,[24] algebraic mapping is much less sensitive than domain truncation to the precise value of L or $\delta_\pm$. Moreover, for functions decreasing as e^{-cx} at infinity (the behaviour we expect for the solution of the flame propagation problem) both techniques give the same rate of convergence.[24]

3.2. Application to flame computations

3.2.1. Problem formulation. Let us consider a flame front propagating in a two-dimensional tube of infinite extent in the direction of propagation of the front. For simplicity we assume that the

combustion processes can be described by an overall one-step exothermic reaction and that the combustible mixture is composed of a homogeneous gas H containing only small traces of a reacting gas R. Therefore the thermal conductivity λ, specific heat C_p and molecular weight of the mixture may be considered as those of the gas H, while the only diffusion coefficient that is to be considered is the binary diffusion coefficient D of R in H. We make the usual assumption of constant thermal conductivity λ, specific heat C_p and Lewis number $Le=\lambda/\rho C_p D$. Considering that the combustion process is an isobaric one, the species and energy conservation equations are

$$\rho C_p \frac{\partial T}{\partial t}+\rho C_p V\cdot\nabla T=\lambda\Delta T+Q\omega, \tag{25}$$

$$\rho\frac{\partial Y}{\partial t}+\rho V\cdot\nabla Y=\frac{\lambda}{C_p Le}\Delta Y-\omega. \tag{26}$$

Here t is the time, Y is the mass fraction of the limiting component R, V is the velocity, ρ is the density of the mixture, Q is the heat of reaction and ω is the reaction rate given by the Arrhenius law

$$\omega=\rho B Y\exp\left(-\frac{E}{R^0 T}\right), \tag{27}$$

where B is the frequency factor, taken here as a constant, R^0 is the universal gas constant and E is the activation energy.

In this paper use will be made of the thermodiffusive model and thus we shall neglect the density change across the flame front and make the assumption $\rho=$constant in equations (25) and (26). Therefore there is no longer a coupling mechanism between the velocity field and the heat release, and the velocity of the gases remains identically equal to zero as the flame front propagates through them.

Introducing U, the normal propagation velocity of the planar deflagration wave, we take as units of time and length $t_0=\lambda/\rho U^2 C_p$ and $l_0=\lambda/\rho U C_p$. With these units the equations (25)–(27) take the form

$$\begin{aligned}\frac{\partial\theta}{\partial t}&=\Delta\theta+\omega,\\ \frac{\partial Y}{\partial t}&=\frac{1}{Le}\Delta Y-\omega,\\ \omega&=A\beta^2 Y\exp\left(\frac{\beta(\theta-1)}{1+\alpha(\theta-1)}\right),\end{aligned} \tag{28}$$

where Y stands now for the non-dimensional mass fraction Y/Y_u, with Y_u the mass fraction of the reactant R in the fresh gases, θ is the reduced temperature $\theta=(T-T_u)/(T_b-T_u)$, with T_b the adiabatic flame temperature given by $T_b=T_u+(Q/C_p)Y_u$, β is the Zel'dovich number equal to $(E/R^0T_b^2)(T_b-T_u)$, α is the thermal expansion parameter $(T_b-T_u)/T_b$ and A has the value

$$A=\frac{\lambda\rho B}{(\rho U)^2 C_p}\frac{e^{(-E/R^0T_b)}}{\beta^2}. \tag{29}$$

In the limit of infinite activation energy, asymptotic methods give[26]

$$A=\frac{1}{2Le}\left(1+\frac{2(3\alpha-2{\cdot}344+Le)}{\beta}\right)+O(\beta^{-2}). \tag{30}$$

In this study we shall use the first-order value for the parameter A:

$$A=\frac{1}{2Le}. \tag{31}$$

For finite (but large) values of the activation energy, this simply implies that the propagation velocity of the one-dimensional deflagration wave is slightly different from unity. In the following section we shall use the numerical method described in Section 2 to compute this deviation and compare it with the value obtained from (29) and (30).

3.2.2. One-dimensional flame propagation. Spectral multidomain methods are just at the beginning of their development and so far the only application to reactive flows seems to be the recent work of Macaraeg *et al.*[27] on the calculation of a one-dimensional shock wave flow with chemical reactions. Here we apply the Chebyshev multidomain method to the computation of flames described by the one-dimensional version of equations (28). Let U be the normal propagation velocity of the planar deflagration wave. In a reference frame moving with speed U, the steady state form of equations (28) is

$$-U\frac{\partial\theta}{\partial x}=\frac{\partial^2\theta}{\partial x^2}+\omega, \tag{32}$$

$$-U\frac{\partial Y}{\partial x}=\frac{1}{Le}\frac{\partial^2 Y}{\partial x^2}-\omega, \tag{33}$$

which gives the relation

$$U=-\int_{-\infty}^{+\infty}\omega\mathrm{d}x. \tag{34}$$

The solution of (32), (33) is computed by the following procedure. The numerical method described in Section 2 is applied to equations (28) where at each time step the two points x_1 and x_2 delimiting the inner domain move with a velocity defined by the integral (34). Appendix I details the numerical evaluation of this integral. This procedure allows us to keep the moving flame front in a well resolved region. The initial conditions are chosen as the asymptotic steady solutions of (32), (33):

$$\begin{aligned}
&\theta(x,0) = \mathrm{e}^{x} && \text{if } x\leqslant 0,\\
&\theta(x,0) = 1 && \text{otherwise},\\
&Y(x,0) = 1-\mathrm{e}^{Le\,x} && \text{if } x\leqslant 0,\\
&Y(x,0) = 0 && \text{otherwise}
\end{aligned} \tag{35}$$

and the computation is performed until the residual defined by

$$R=\max\left\{\sup_{i,j}\frac{|\theta^{n+1}(i,j)-\theta^{n}(i,j)|}{\delta t},\ \sup_{i,j}\frac{|Y^{n+1}(i,j)-Y^{n}(i,j)|}{\delta t}\right\}, \tag{36}$$

where $\sup_{i,j}$ denotes the maximum value over all the collocation nodes, becomes smaller than a given threshold.

In all the computations reported below, the thermal expansion parameter is given the value $\alpha=0{\cdot}8$ and δt is equal to 10^{-2}. The following discretization is used: $N_-=N_+=24$, $N_0=36$ and $\delta_0=x_2-x_1=1$. In order to simulate a one-dimensional computation, we have used the value $M=3$. Figure 2 shows the temperature and reaction rate profiles obtained at steady state for the

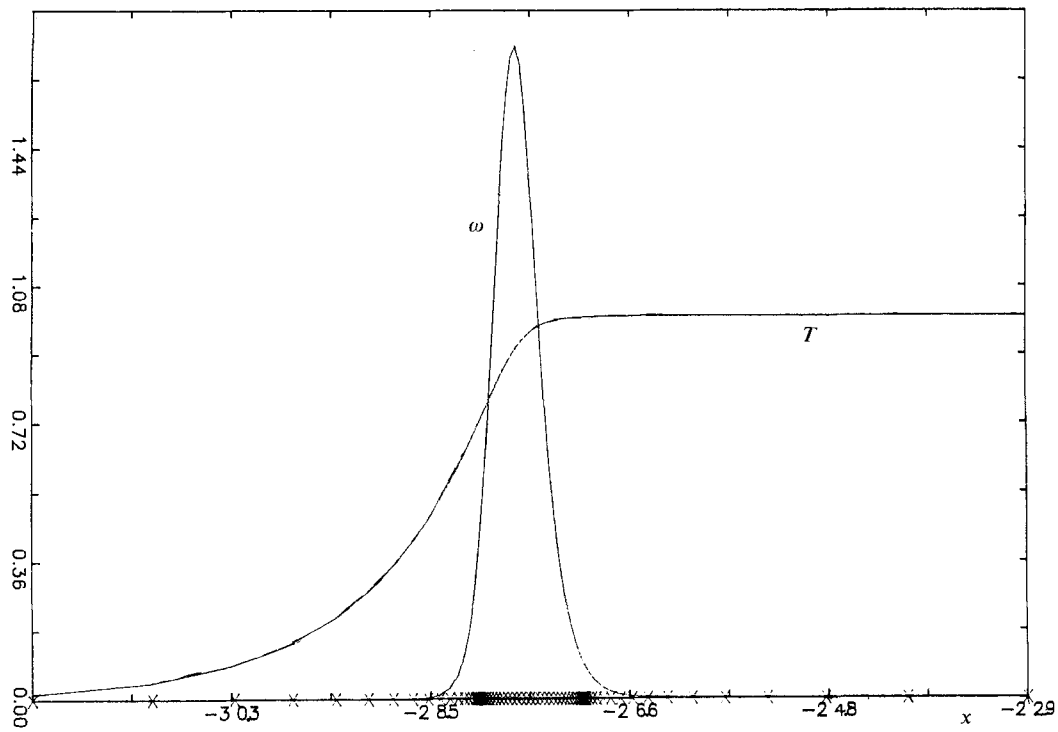

Figure 2. Temperature and reaction rate profiles with the discretization $N_- = 24$, $N_+ = 24$ and $N_0 = 36$

following values of the parameters: $\beta = 10$ and $Le = 1$. The distribution of the collocation points resulting from the multidomain approach is displayed on the x-axis. One can see that the collocation points are clustered in the flame front, providing a very good resolution of this region; as a result no oscillations appear in the computed profiles. The result of another computation performed with the following values of the discretization parameters—$N_- = 20$, $N_0 = 36$, $N_+ = 8$ and $\delta_0 = x_2 - x_1 = 1{\cdot}5$—is shown in Figure 3. This result compares very well with that previously obtained with a finer discretization; in particular the values of the flame velocity (which is the fundamental unknown of this problem) differ by less than 10^{-4}. This proves that for this problem the discretization in the outer domain can be rather coarse provided the flame front region is well represented. One can see that the profiles of Figure 3 are slightly offset relative to those of Figure 2; however, instead of a loss of accuracy in the computation of the flame velocity, this is rather due to an initial shifting and deformation of the asymptotic profiles (35) which appear at the beginning of the time integration and depend on the resolution of the flame front as well as on the initial location of the inner domain (which was different in the two calculations).

We now compare the values of the computed flame velocity with those obtained by asymptotic analysis for different values of the physical parameters. The asymptotic results are reported from Reference 28.

(a) $Le = 0{\cdot}5$, $\beta = 10$: the asymptotic velocity is $U_a = 0{\cdot}946$, the computed velocity is $U_c = 0{\cdot}949$.
(b) $Le = 1$, $\beta = 10$: the asymptotic velocity is $U_a = 0{\cdot}9$, the computed velocity is $U_c = 0{\cdot}917$.
(c) $Le = 1$, $\beta = 20$: the asymptotic velocity is $U_a = 0{\cdot}949$, the computed velocity is $U_c = 0{\cdot}953$.

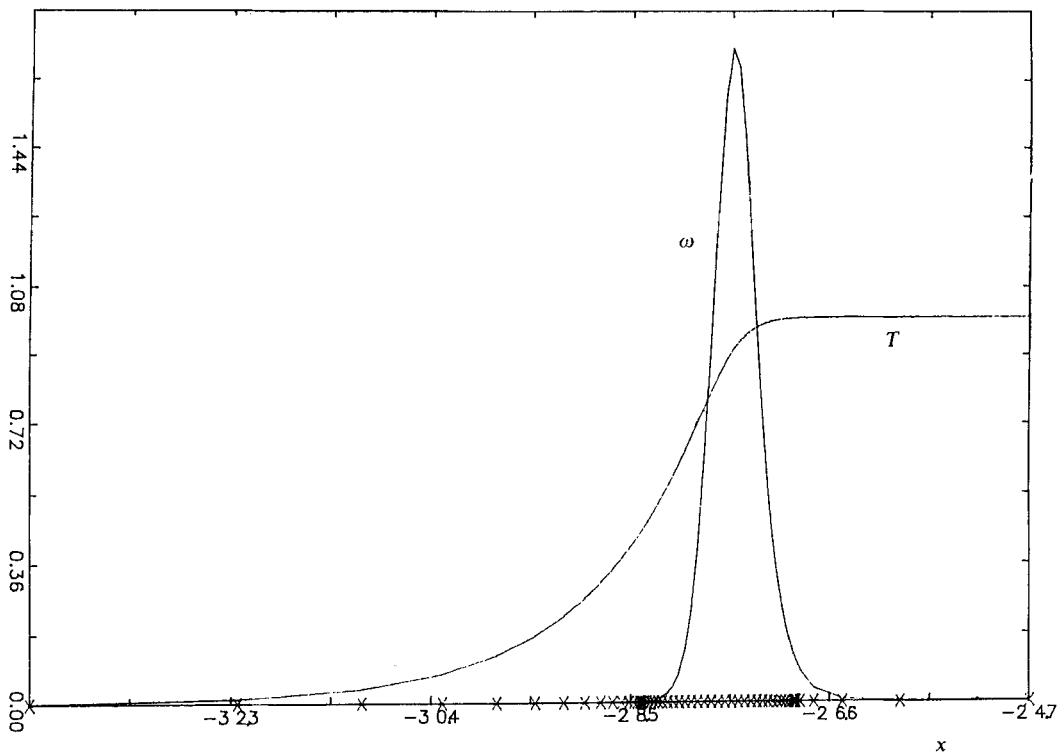

Figure 3. Temperature and reaction rate profiles with the discretization $N_- = 20$, $N_+ = 8$ and $N_0 = 36$

We note a good agreement between the computed and asymptotic velocities. Comparison of the present results with the values obtained by finite difference methods reported in Reference 28 also shows good agreement.

3.2.3. Stability of a plane flame front. In this section we shall examine the problem of the stability of a two-dimensional flame front described by (28) travelling in a channel of width $2a$. The computation of such flames is made delicate because the instabilities occur on a time scale much larger than the flame transit time (defined as the ratio of the asymptotic flame thickness to the asymptotic flame velocity) and thus requires an efficient (implicit) time stepping to keep the computational cost within reasonable bounds. Moreover, the instabilities occur only if the width of the channel is large enough with respect to the flame thickness; thus it is necessary to use an accurate spatial approximation in order to keep a good resolution in the transverse direction.

In the limit of large activation energy, the asymptotic study of this problem performed by Sivashinsky[29] shows that the behaviour of the front is governed by the parameter η defined by

$$\eta = \frac{\beta}{2}(1 - Le).$$

A linear stability analysis leads to the dispersion relationship

$$\gamma = (\eta - 1 - 4\eta^2 k^2)k^2, \tag{37}$$

where γ is the amplification factor and k is the wave number of the perturbation. We can deduce from (37) that for $\eta \leqslant 1$ all perturbations are damped out and the flame front is stable, while for $\eta \geqslant 1$ there exists a range of unstable wave numbers from $k=0$ to $k_0=(\eta-1)^{1/2}/2\eta$ with a maximum value of γ obtained for $k_c=k_0/2\sqrt{2}$.

This theory is now tested numerically using the algorithm described in Section 2. Similar computations using different numerical methods are reported in References 8, 30 and 31. The initial conditions are chosen to have the form

$$\begin{aligned} \theta(x, y, 0) &= \exp(x-f(y)) && \text{if} \quad x \leqslant f(y), \\ \theta(x, y, 0) &= 1 && \text{if} \quad x \geqslant f(y), \\ Y(x, y, 0) &= \exp[Le(x-f(y))] && \text{if} \quad x \leqslant f(y), \\ Y(x, y, 0) &= 0 && \text{if} \quad x \geqslant f(y), \end{aligned} \tag{38}$$

with $f(y)=0{\cdot}5\cos(2\pi y/\lambda)$, and represent a flame front perturbed with a wavelength of value λ, while the boundary conditions are

$$\begin{aligned} \theta &\to 0 \quad \text{for} \quad x \to -\infty, \\ \theta &\to 1 \quad \text{for} \quad x \to +\infty, \\ (\partial\theta/\partial y) &= 0 \quad \text{at} \quad y \pm a, \\ Y &\to 1 \quad \text{for} \quad x \to -\infty, \\ Y &\to 0 \quad \text{for} \quad x \to +\infty, \\ (\partial Y/\partial y) &= 0 \quad \text{at} \quad y \pm a. \end{aligned} \tag{39}$$

We choose $\beta=10$ and $Le=0{\cdot}7$; thus according to equation (37) the range of unstable wavelengths is equal to the interval $[6\sqrt{2}\pi, +\infty]$.

All the calculations reported below have been done with the following values of the discretization parameters—$N_-=N_+=20$, $N_0=36$ and $M=64$, $\delta_+=\delta_-=1$—and the time step is given the value $\delta t=10^{-2}$. We first consider $\lambda=2\pi$. In this case the dimension of the inner domain, $\delta_0=x_2-x_1$, is equal to 1·5. Figure 4 displays the evolution of the isotherms. As predicted by relation (37), the initially wrinkled flame relaxes to a plane one.

Next we consider $\lambda=2\pi/k_0$, the limit of unstable wavelength. The dimension of the inner domain is again chosen equal to 1·5. Figure 5 shows the evolution of the isotherms. The computation has been performed up to the time $t=100$ and shows as in Reference 31 the development of a wrinkled flame front reaching a near steady state.

Finally we have considered the value $\lambda=2\pi/k_c$, which corresponds to the maximum amplification factor. As we expect the development of large cusps of the flame front in this case, the dimension of the inner domain is somewhat larger than in the previous case and is here chosen to be equal to 1·8. Figure 6 displays the evolution of the isotherms up to the time $t=100$ and shows the rapid development of the perturbation. We may observe in Figures 5 and 6 that the flame front is not entirely enclosed within the inner domain, although the region of large gradient is effectively within the inner domain; the part of the front that lies outside the inner domain is less steep and also benefits to some extent from the natural clustering of the Chelbyshev collocation points near a boundary.

4. CONCLUSIONS

A Chebyshev collocation method has been proposed for the computation of laminar flame propagation in a two-dimensional gaseous medium. The principal difficulty in such computations

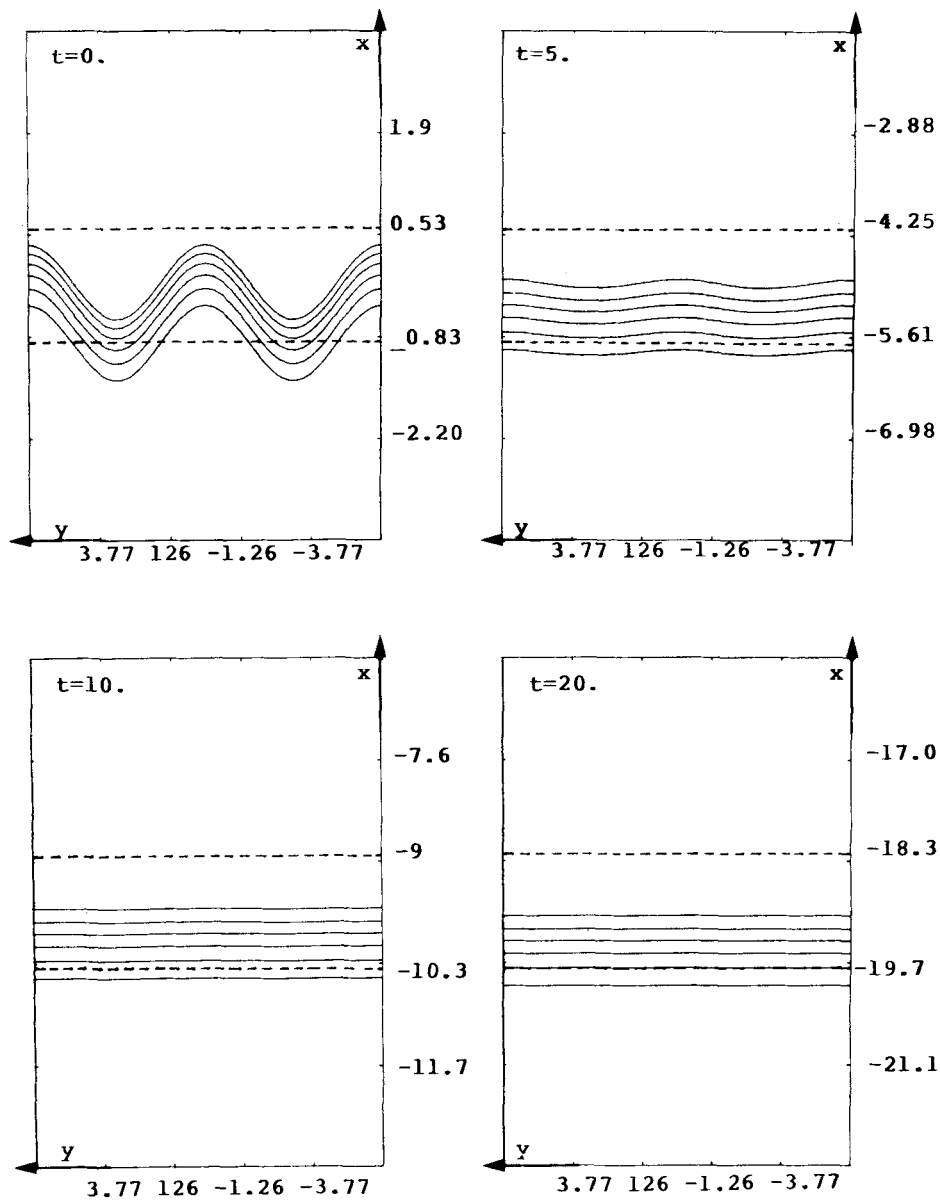

Figure 4. Evolution of the isotherms. The dashed lines indicate the location of the inner domain. $\lambda = 2\pi$

comes from the presence well inside the domain of a zone of large variations of the variables uneasily represented by classical Chebyshev methods.

One possible solution was investigated in Reference 8. There the use of a co-ordinate transform to concentrate the collocation points in the flame front was advocated. However, in the case of moving interfaces this requires us to define a time-dependent co-ordinate transform which changes as the computed solution evolves. Such a self-adaptive mapping can be defined based on a minimization procedure such as that of Reference 8.

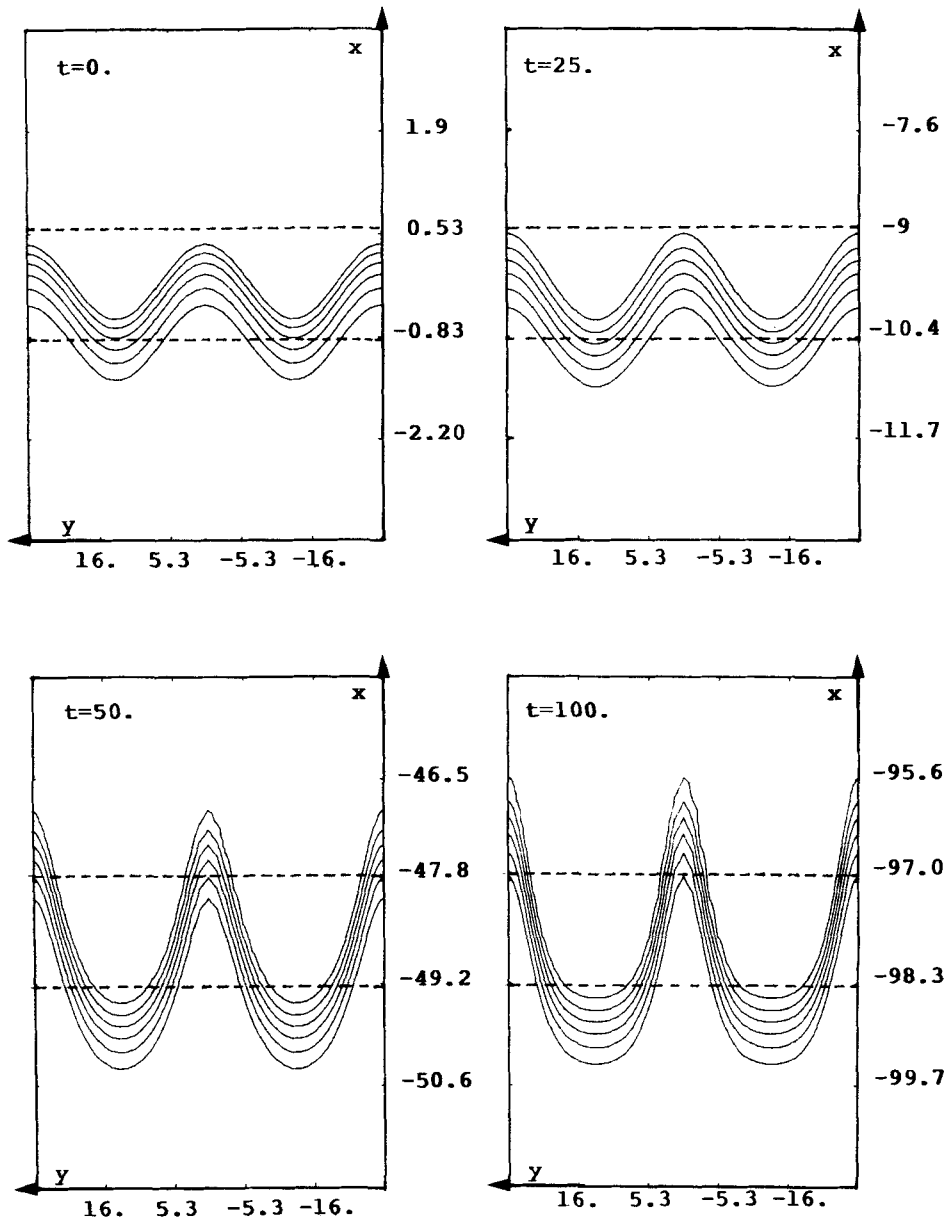

Figure 5. Evolution of the isotherms. The dashed lines indicate the location of the inner domain. $\lambda = 2\pi/k_0$

Here we have investigated another solution is which the desired accuracy in the flame front is obtained by a multidomain method. In this decomposition technique the flame front is approximately enclosed in a moving subdomain which follows the flame front in its movement. The continuity conditions at the interfaces are enforced by an influence matrix technique and the two infinite outer subdomains are mapped into finite computational domains. The efficiency of this method lies in the fact that after a preprocessing stage all the computational effort is reduced at each time step to matrix products.

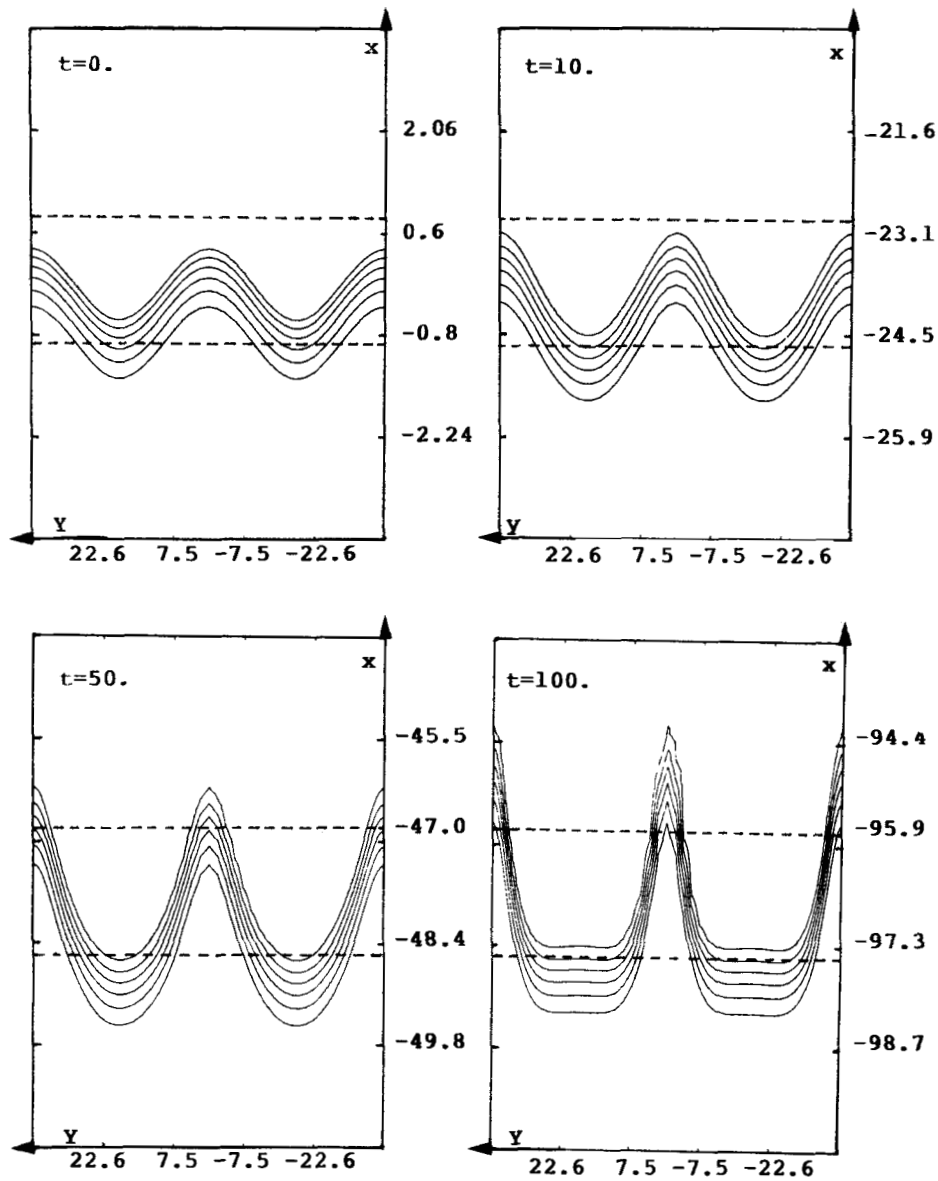

Figure 6. Evolution of the isotherms. The dashed lines indicate the location of the inner domain $\lambda = 2\pi/k_c$

A thorough comparison of the efficiency of the two methods is difficult since both methods are still in development. For the special case treated in this paper, both methods give accurate results and seem of comparable efficiency (note that a Fourier–Chebyshev approximation was used in Reference 8 instead of a Chebyshev–Chebyshev approximation). However, the multidomain method seems of more general applicability when the interfaces or the geometry are complicated. A very interesting direction would be to combine the two methods to benefit from both their advantages. This is likely to be the most promising way to construct versatile Chebyshev collocation methods for solving more general moving front and interface problems.

ACKNOWLEDGEMENT

The computations reported above were made possible by a grant from 'Centre de Calcul Vectoriel pour la Recherche'.

APPENDIX

The velocity $U(t)$ is defined by

$$U = -\frac{1}{2a}\int_{-\infty}^{+\infty}\int_{-a}^{a} \omega \mathrm{d}x\,\mathrm{d}y, \tag{40}$$

which becomes in the transformed co-ordinate system

$$U = \frac{1}{2}\sum_{j\in\{-,0,+\}}\int_{-1}^{+1}\int_{-1}^{1} q_j\omega_j \mathrm{d}\xi\mathrm{d}\eta, \tag{41}$$

where q_j is a function of ξ coming from the change of variable. Knowing the values of the functions $q_j\omega_j$ at the collocation points, we can define their interpolation polynomials by a double Chebyshev expansion. Then the integration is performed term by term using the classical formulae for integration of the Chebyshev polynomials on $[-1, +1]$.

REFERENCES

1. D. Gottlieb and S. A. Orszag, 'Numerical analysis of spectral methods: theory and applications', *CBMS Regional Conference Series in Applied Mathematics*, SIAM, Philadelphia, 1977.
2. R. G. Voigt, D. Gottlieb and Y. Hussaini (eds), *Spectral Methods for Partial Differential Equations*, SIAM, Philadelphia, 1984.
3. C. Canuto, M. Y. Hussaini, A. Quarteroni and T. A. Zang, 'Spectral methods in fluid dynamics', *Springer Series in Computational Physics*, Springer-Verlag, 1987.
4. E. Tadmor, 'The exponential accuracy of Fourier and Chebyshev differencing methods', *SIAM J. Numer. Anal.*, **23**, 1–10 (1986).
5. S. A. Orszag, 'Spectral methods in complex geometries', *J. Comput. Phys.*, **37**, 70–92 (1980).
6. C. Badesvant, M. Deville, P. Haldenwang, J. M. Lacroix, J. Ouazzani, R. Peyret, P. Orlandi and A. Y. Patera, 'Spectral and finite difference solution of the Burgers equation', *Comput. Fluids*, **14**, 23–41 (1986).
7. M. E. Brachet, 'Simulation numérique directe d'écoulements turbulents tridimensionnels', *Thesis*, University of Nice, 1983.
8. H. Guillard and R. Peyret, 'On the use of spectral methods for stiff problems', *Comput. Methods Appl. Mech. Eng.*, **66**, 17–43 (1988).
9. A. Bayliss and B. J. Matkowsky, 'Fronts, relaxation, oscillations and period doubling in solid fuel combustion', *J. Comput Phys.* **71**, 147–168 (1987).
10. A. Quarteroni, 'Domain decomposition techniques using spectral methods', *Publication No. 540*, Istituto di Analisi Numezica, Pavia, 1986.
11. I. Babuska, B. A. Szabo and I. N. Katz, 'The *p*-version of the finite element method', *SIAM J. Numer. Anal.*, **18**, 515–545 (1981).
12. A. T. Patera, 'A spectral element method for fluid dynamics: laminar flow in a channel expansion', *J. Comput. Phys.*, **54**, 468–488 (1984).
13. L. M. Delves and C. A. Hall, 'An implicit matching procedure for global element calculations', *J. Inst. Math. Appl.* **23**, 223–234 (1979).
14. P. Zanolli, 'Domain decomposition algorithms for spectral methods', *Calcolo*, **24**, 201–240 (1987).
15. D. Funaro, A. Quarteroni and P. Zanolli, 'An iterative procedure with interface relaxation for domain decomposition methods', *Report No. 532*, Instituto di Analisi Numerica, Pavia, 1986.
16. M. Macaraeg and C. L. Streett, 'Improvements in spectral collocation through a multiple domain technique', *Appl. Numer. Math.*, **2**, 95–108 (1986).
17. Y. Marion, 'Méthodes spectrales de décomposition en sous-domaines: application à la résolution des équations de Navier–Stokes instationnaires', *Thesis*, University Claude Bernard, Lyon, 1987.
18. J. P. Pulicani, 'A spectral multi-domain method for the solution of 1-D Helmholtz and Stokes-type equations', *Comput. Fluids.*, **16**, 207–215 (1988).

19. L. Kleiser and U. Schumann, 'Treatment of incompressibility and boundary conditions in 3-D numerical spectral simulations of plane channel flow', in E. H. Hirschel (ed.), *Proc. Third GAMM Confer. Numerical Methods in Fluid Mechanics*, Vieweg, Braunschweig, 1980, pp. 165–173.
20. R. Peyret, 'Introduction to spectral methods', *Von Karman Institute, Lecture Series 1986–04*, 1986.
21. U. Ehrenstein, 'Méthodes spectrals de résolution des équations de Stokes et de Navier–Stokes. Application à des écoulements de convection double-diffusive', *Thesis*, University of Nice, 1986.
22. U. Ehrenstein and R. Peyret, 'A Chebyshev collocation method for the Navier–Stokes equations with application to double-diffusive convection', *Int. j. numer. methods fluids*, **9**(4), 427–452 (1989).
23. P. Haldenwang, G. Labrosse, S. Abboudi and M. Deville, 'Chebyshev 3-D spectral and 2-D pseudospectral solvers for the Helmholtz equation', *J. Comput. Phys.*, **55**, 115–128 (1984).
24. J. P. Boyd, 'The optimization of convergence for Chebyshev polynomial method in an unbounded domain', *J. Comput. Phys.* **45**, 43–79 (1982).
25. C. E. Grosh and S. A. Orszag, 'Numerical solution of problems in unbounded regions: coordinate transforms', *J. Comput. Phys.* **25**, 273–296 (1977).
26. W. B. Bush and F. E. Fendel, 'Asymptotic analysis of laminar flame propagation for general Lewis number', *Combust. Sci. Technol.*, **1**, 421–428 (1970).
27. M. Macaraeg, C. L. Streett and M. Y. Hussaini, 'An analysis of artificial viscosity effects on reacting flows using a spectral multi-domain technique', *ICASE Report No. 87–35*, 1987.
28. N. Peter and J. Warnatz, 'Numerical methods in laminar flame propagation', *Notes on Numerical Fluid Mechanics, Vol. 6*, Vieweg, Braunschweig, 1982.
29. G. I. Sivashinsky, 'Non linear analysis of hydrodynamic instability in laminar flame. I—Derivation of basic equations', *Acta Astron.* **4**, 1177–1206 (1977).
30. F. Benkhaldoun, 'Etude numérique de modèles mathématiques décrivant la propagation de flammes dans un milieu gazeux bidimensionnel', *Thesis*, University of Nice, 1987.
31. H. Guillard, N. Maman and B. Larrouturou, 'Etude numérique des instabilités cellulaires d'un front de flamme par une méthode pseudo-spectrale', *INRIA Report No. 721*, 1987.